ACS Macro Letters

Letter

pubs.acs.org/macroletters

Thermoelectrical Memory of Polymer Nanocomposites

Fabienne Grillard,[†] Philippe Poulin,[†] Alexander Korzhenko,[‡] Patrice Gaillard,[‡] and Cécile Zakri*[,†]

[†]Université de Bordeaux, CNRS, Centre de Recherche Paul Pascal, 115 Avenue Schweitzer, 33600 Pessac, France

[‡]Groupement de Recherches de Lacq, Arkema, BP 34 Lacq 64170, France

ABSTRACT: The inclusion of nanoparticles improves the behavior of shape-memory polymers and allows new functionalities. It is shown in the present work that polyamide fibers loaded with carbon nanotubes (CNTs) exhibit novel memory functions associated to their electrical conductivity. Similar to classical shape memory polymers, the materials are predeformed at high temperature and then quenched down to room temperature and subsequently reheated. Their resistivity is recorded during the process and is found to decrease with temperature during the last heating stage. The rate of resistivity decrease exhibits a well-defined maximum at the temperature of predeformation. This unique response clearly shows an accurate thermoelectrical material memory. Temperature memory extended to electrical properties could serve for future sensing applications coupled to shape changes.

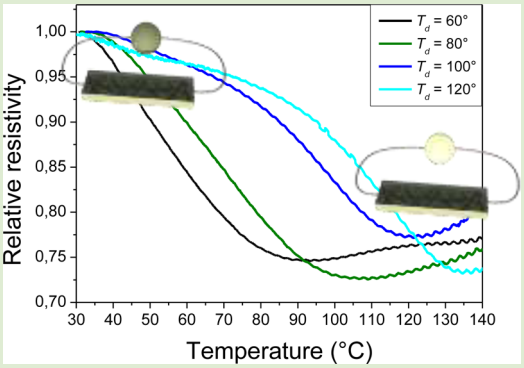

Thermoinduced shape-memory materials are able to fully or partially revert to their original shape after being manipulated at different temperatures to different shapes. They are generally made of polymers[1] or metallic alloys.[2] Shape-memory materials can generate various levels of strain and stress recovery.[3,4] Compared to metals, shape-memory polymers (SMPs) exhibit unique features including large strain deformation and the capability to memorize the temperature at which they have been initially deformed.[5−7] Some materials can memorize two or several shapes,[8−10] thus showing the versatility of polymers and their strong potential for applications in medical devices, heat shrink tubing, deployable aerospace and aircraft structures, microdevices, MEMS, toys, etc. The inclusion of nanoparticles has also been proved to improve the behavior of shape-memory polymers.[11−14] This in addition can increase their mechanical properties[15] and allows shape-memory effects triggered by external fields.[12,16]

In all the above-mentioned cases, the involved thermal transitions are revealed by the generation of mechanical stress and deformations of the materials. These phenomena are due at a microscopic level to the storage and relaxation of mechanical energy by the polymer chains as the temperature is varied.[17−19] It can be expected that properties other than mechanical properties are affected by such mechanisms. Variations of such properties could serve as new types of memories in polymer materials and provide therefore new functionalities for sensing or other potential applications.[20] However, investigation of observables other than the mechanical response remains challenging. This is in part due to the fact that most SMPs do not display large panels of functionalities, but the development of polymer-based nanocomposites is a way to achieve polymer materials with additional properties[21] and offers therefore a route toward the exploration of new memory behavior in polymer systems.

We investigate in the present work, polymer fibers loaded with carbon nanotubes (CNTs). Such fibers are electrically conductive. They are predeformed at different temperatures between 60 and 120 °C. Then, predeformed fibers are cooled down at fixed strain and reheated to high temperature in a so-called reading stage. Their resistance is recorded as a function of temperature during the whole process. It is found to decrease with temperature during the reading stage, and the rate of resistivity decrease exhibits a well-defined maximum at the temperature of predeformation. Thus the response of the fibers clearly shows a new and accurate thermoelectrical memory, through which the materials can communicate the exact temperature at which it was initially processed. The underlying mechanisms are discussed by considering structural characterizations.

Figure 1 shows the resistivity and mechanical stress of PA12 fibers, containing 7 wt % of CNTs, during the predeformation step, as a function of strain and for different temperatures. The stress versus strain curves show the thermal softening of the fibers with temperature. Indeed a lower stress is needed to reach a given strain with increasing temperatures. By contrast, resistance changes as a function of strain do not strongly depend on temperature. Whatever the temperature, a slight and almost linear increase of the resistivity is observed at small strain in the elastic regime of deformation (see inset in Figure 1). A larger increase of resistivity is found at greater strain up to 200% in the regime of plastic deformation. This level of stretching induces an increase of resistivity by almost an order of magnitude.

Received: December 12, 2013
Accepted: February 3, 2014
Published: February 17, 2014

   dx.doi.org/10.1021/mz400637d | *ACS Macro Lett.* 2014, 3, 224−228

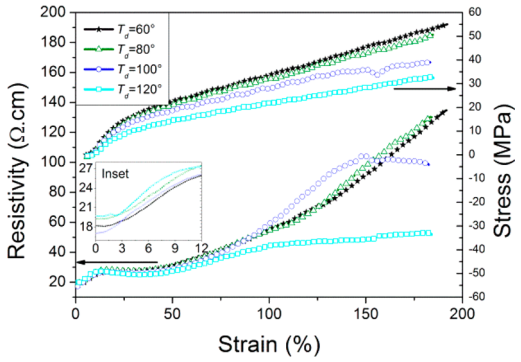

Figure 1. Stress and resistivity of PA12 fibers, containing 7 wt % of CNTs, as a function of strain at different deformation temperatures (T_d) indicated in the graph. Inset: zoom of the resistivity curves at low strain.

The increase of resistivity can be ascribed to the disruption of the conductive network formed by nanotubes and nanotube aggregates. Previous studies have shown that in the case of very large strain up to 2000% this disruption is essentially dominated by the relative translation of the CNTs with respect to each other. This induces losses of electrical contacts and a quadratic-like increase of the resistivity as a function of strain.[22] In the present work, the level of strain is much smaller than 2000%, but the resistivity increase is still observed. Nevertheless, its quantitative amplitude is found to vary from a sample to another in a nonsystematic way. This is likely due to different morphologies of networks formed by CNTs and CNT aggregates within the fibers. These differences, which are not controlled, could explain variability of the resistivity in the intermediate regime of network disruption of the present study. However, as discussed below, the phenomenon of interest deals with relative variations of resistivity as a function of temperature, regardless of the net values.

The 200% stretched fibers are subsequently cooled to room temperature at fixed strain.

They are then reheated from room temperature to high temperature, up to 150 °C. Their resistance is recorded as a function of temperature. The graph in Figure 2(a) shows the relative resistivity of the fibers, i.e., the ratio between the resistivity at a given temperature T and the resistivity at room temperature. The derivative of the resistivity versus the temperature $d\rho/dT$ is shown in Figure 2(b).

The qualitative behavior of fibers predeformed at distinct temperatures T_d is the same. The fiber resistivity decreases progressively with temperature, until it reaches a minimum value. The curves show an inflection point for which the rate of resistivity decrease is the largest. The net relative resistivity loss is about 25% and is independent of the temperature at which the fiber has been deformed. This behavior is surprising at first sight and is discussed below. However, the temperature at which the resistivity falls down varies strongly with the predeformation temperature T_d. This effect reveals a memory behavior since the electrical properties of the fibers depend on their processing history. The degree of memorization can be more clearly visualized by looking at the derivative of the resistivity. The inflection points appear now as minima. As shown in Figure 2(c), the temperature of these minima is reproducibly close to the temperature T_d. The present thermoelectrical memory is therefore accurate since the materials can communicate via its changes of resistance the

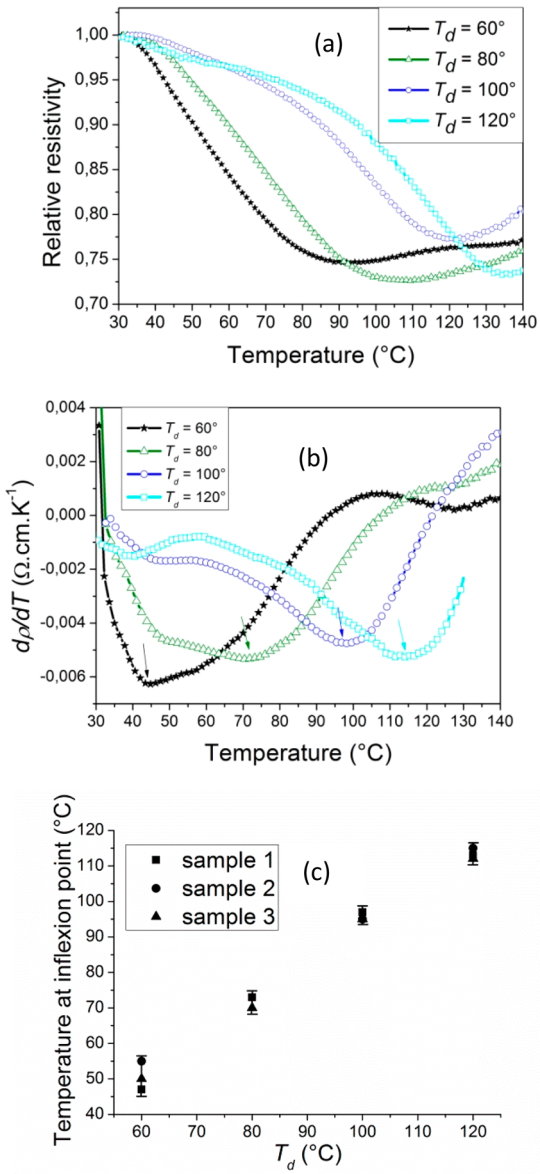

Figure 2. (a) Relative resistivity and (b) derivative of the resistivity as a function of temperature of PA12 fibers, containing 7 wt % of CNTs and predeformed at 200% and at different deformation temperatures (T_d) as indicated in the graph. (c) Temperatures at inflection points versus deformation temperatures for a set of three different samples (labeled 1, 2, and 3) of the same fiber, showing the reproducibility of the thermoelectrical memory.

temperature at which it was processed before being quenched and stored at room temperature. This phenomenon appears as the electrical parallel of the mechanical temperature memory effects (TMEs) observed in shape-memory polymers.[5,17−19]

The observed thermoelectrical memory is therefore likely arising from relaxation phenomena that are also involved in TMEs. Structural characterizations have been performed to gain more insights into the mechanisms at the origin of the present changes of resistivity. The latter are related to changes of the quality or of the number of contacts between nanotubes within the fiber. Variations of resistivity are not likely due to a translation of the nanotubes because the fiber length is kept fixed during the measurement. Nevertheless, thermomechanical relaxations associated to the release of stress of the polymer are occurring[5] when the temperature rises. These relaxations are

dx.doi.org/10.1021/mz400637d | ACS Macro Lett. 2014, 3, 224−228

associated to a gain in mobility of the polymer chains with a release of mechanical stress. Such phenomena can alter the conductivity of the nanocomposites via at least two main mechanisms. First, changes of the CNT orientation can lead to variations of the contact density and therefore to variations of the electrical conductivity. Indeed, CNTs can be expected to rotate during predeformation of the fibers at high temperature. After quenching the CNTs remain locked and partially aligned in the glassy polymer. This orientation is associated to an unstable state of the polymer. It can therefore be expected that the orientation of the CNTs can diminish when they are unlocked with increasing temperature. A loss of orientation should be associated to an increase of their contact probability[23,24] and therefore to a decrease of resistivity of the nanocomposites. Second, polymer chains in between neighboring nanotubes can move and be expelled from the interface of the CNTs so that the latter can approach each other in response to strong van der Waals interactions. Minute variations of the spacing between two CNTs can have a strong effect on the conductivity because the tunnelling contact resistance between two CNTs varies exponentially as a function of the separation between the CNT interfaces.[25−28]

Orientation of the CNTs within the fibers at different steps of the process has been characterized by SAXS experiments to clarify the dominant mechanism. The experiments were performed for fibers predeformed at 60 °C (black lines in Figures 1 and 2). A 2D SAXS pattern is first recorded on a raw fiber before any treatment. This pattern serves as a reference (Figure 3(a)). Then a pattern of a fiber that has been stretched at 60 °C to 200% is measured (Figure 3(b)). Lastly, this predeformed fiber is reheated up to high temperature at 150 °C, and its SAXS pattern is recorded and shown (Figure 3(c)). Corresponding X-ray spectra of the scattered intensity as a function of the wave vector are shown in Figure 3(d). Classical diffraction peaks of the PA12[29,30] and of the CNTs[31] are observed. In particular, the [0 0 2] diffraction peak of the CNTs is at a wave vector of 1.85 Å^{-1}. These peaks are of weak intensity because of the nonperfect graphitized structure of the CNTs and of their diameter of finite size but remain well measurable above the noise of the measurements (see inset in Figure 3).

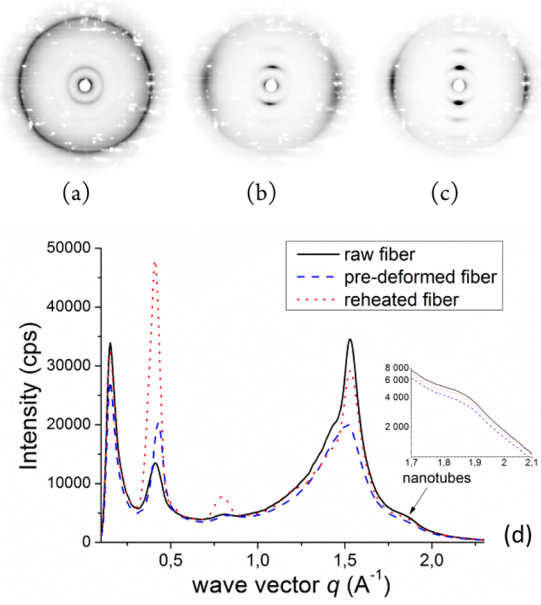

Figure 3. SAXS bidimensional patterns of a PA12 fiber, containing 7 wt % of CNTs, before any treatment (a), after 200% predeformation at 60 °C (b), and after reheating up to 150 °C (c). (d) X-ray corresponding spectra. Inset: zoom of the data that shows the scattering signal of the nanotubes.

The pattern in Figure 3(a) reveals that there is no or very little degree of alignment in raw fibers. By contrast, the anisotropic patterns in Figure 3(b) and Figure 3(c) clearly reveal an orientation of the PA12 and of the CNTs after stretching. Following approaches already detailed in the literature, the angular distribution of the scattered intensity at 1.85 Å^{-1} is calculated to quantify the degree of orientation of the CNTs.[32,33] The same approach was used for the intensity at 1.53 Å^{-1} associated to the [0 0 1] peak of a crystalline form of PA12.[29,30] The obtained distributions were fitted by Gaussian functions. The half width at half-maximum (HWHM) of the Gaussian functions is taken as the degree of orientation of the CNTs and of the polymer.

The HWHM values are reported in Table 1. Before any predeformation (Figure 3 (a)), and as expected at first sight from the 2D SAXS patterns, CNTs and PA12 are randomly oriented, the angular scattered intensity at 1.85 Å^{-1} and at 1.53 Å^{-1} being isotropic. After stretching to 200% at 60 °C, a significant gain of alignment of the nanotubes and the polymer chains is observed. The degrees of alignment, respectively, are of 33° and 20° (Figure 3(b)), but the orientation of the CNTs decreases to 37° when the fiber is reheated to 150 °C (Figure 3(c)). By contrast, the polymer chain alignment is improved after this treatment with a HWHM of 14°.

Table 1. Values of HWHM Deduced from the X-ray Data of Figure 3, Representing the Mean Orientation of Nanotubes and Polymer Chains within a Fiber at Different Steps of Their Processing

	HWHM (deg)	
	nanotubes	polymer
raw fiber	isotropic	isotropic
predeformed fiber (60 °C, 200%)	33	20
reheated fiber (150 °C, fixed)	37	14

Figure 2 shows a decrease of resistivity of about 25% after reheating. A loss of alignment increases the excluded volume of the nanotubes and thereby their contact probability.[24,34] A higher number of intertube contacts is expected to improve the conductivity of the material as experimentally qualitatively observed. The excluded volume V_{ex} of a cylindrical particle of length L and diameter d is given by[35]

$$\langle V_{ex}\rangle = \frac{4\pi}{3}d^3 + 2\pi L d^2 + 2L^2 d\langle \sin(\gamma)\rangle$$

In this expression, γ represents the angle formed by two particles in the material.

In the case of nanotubes, where $L \gg d$, the excluded volume can be simplified to

$$\langle V_{ex}\rangle \approx 2L^2 d\langle \sin(\gamma)\rangle$$

Thus, a variation of the mean orientation from ±33 to ±37° leads to an increase of the excluded volume by only 5%. In this rough estimation, γ is assimilated to the full width at half-maximum of the X-ray distribution.[22] Assuming that the conductivity is proportional to the number of intertube

dx.doi.org/10.1021/mz400637d | ACS Macro Lett. 2014, 3, 224−228

contacts and thus to the excluded volume, it can be concluded that the disorientation of the nanotubes cannot explain variations of conductivity substantially greater than 5%. As indicated above, reheating leads to a decrease of resistivity by about 25%. This decrease is therefore more likely due to minute changes of the structure of the intertube contacts rather than to large changes of the CNT orientation. The observation that the net relative resistivity loss does not strongly vary with temperature also suggests that the change of spacing between the CNTs remains comparable for relaxations at different temperatures.

The inclusion of CNTs within PA12 allows the fabrication of electrically conductive fibers by melt spinning. These fibers have shape-memory properties associated to thermally induced relaxation mechanisms. In particular, the present fibers exhibit a thermoelectrical memory characterized by changes of electrical properties at temperatures that can be tuned by the programming process of the material.

These composite materials are thus ideal candidates for the development of shape-memory devices, in which the shape recovery is coupled with new functionalities like resistance changes.

EXPERIMENTAL SECTION

Neat and composite fibers are made of polyamide 12 (PA12 AMNO TLD-grade Arkema) and multiwall carbon nanotubes (C100-Graphistrength Arkema) produced by a catalyzed chemical vapor deposition process. The glass transition and melting temperatures of the polymer are, respectively, 55 and 180 °C. The CNTs have an average external diameter of 10−15 nm and a length of several micrometers. They are used without purification or surface treatment. The fibers are spun by a melt spinning process already described in the literature.[22,36] The composite fibers contain 7 wt % of CNT. Before processing, neat PA12 or PA12−CNT blends are dried overnight at 80 °C in vacuum. The dried materials are introduced in a Scamex single screw extruder and heated to 250 °C, a temperature well above the melting temperature of the polymer. The molten polymer is forced through a cylindrical spinneret with a 0.5 mm diameter. The screw extruder velocity is set to 30 rpm to control the supply rate of polymer. The extruded filament is wound up around the rollers of a drawing bench at a constant take-up velocity. The linear velocity of the rolls is set to 27.5 m/min. The diameter of the resultant fibers is about 250 μm.

Thermoelectrical memory experiments are performed in a tensile load Zwick BTC-FR2.5TN.D09 setup, with a controlled temperature oven as detailed in other studies of shape-memory materials.[22,37] The fiber is connected by silver paste contacts to a Keithley 2000 multimeter so that its electrical resistance can be measured during deformations and/or temperature changes. A fiber of initial length l_0 is predeformed at a constant temperature, T_d, between the polymer glass transition temperature T_g and the polymer melting transition temperature T_m. The deformation is performed at a constant speed of 1.2 mm/min, and the maximum strain is 200%. Typically, the initial length of the fiber is 10 mm. During this programming step, the electrical resistance of the fiber is measured as a function of strain, the strain being defined as $\varepsilon = (l - l_0)/l_0$, where l is the length of the deformed fiber.

The resistivity is deduced from $\rho = RS/\lambda$, where S is the cross section of the fiber and λ the distance between the two electrodes. Variations of S and λ during deformations are taken into account. These variations are coupled by considering that the volume of the fiber remains constant. The material is quickly quenched to room temperature at fixed length after having being stretched at high temperature. The polymer is at this stage in its glassy state. After cooling, remaining stress is released by slightly approaching the clamps of the setup to reduce the strain.

The thermoelectrical memory is characterized as the fiber is reheated from room temperature to a temperature above T_d in isometric conditions, i.e. at fixed length during this temperature scanning. Small-angle X-ray scattering characterisations are performed to investigate the orientation of the nanotubes within the fiber. A Nanostar Bruker diffractometer equipped with a 2D detector is used. Fibers are fixed horizontally on a special holder. The diffraction peak at 1.85 Å^{-1}, which is related to the spacing of the graphite [0 0 2] layers, is used to deduce the orientation of the nanotubes. The angular distribution of the scattered intensity at this wave vector is fitted by a Gaussian function. The degree of alignment of the nanotubes is directly deduced from the half width at half-maximum (HWHM) of the Gaussian function.[37]

AUTHOR INFORMATION

Corresponding Author

*E-mail: zakri@crpp-bordeaux.cnrs.fr.

Notes

The authors declare no competing financial interest.

REFERENCES

(1) Behl, M.; Razzaq, M. Y.; Lendlein, A. *Adv. Mater.* **2010**, *22*, 3388−3410.
(2) Van Humbeeck, J. *Adv. Eng. Mater.* **2001**, *3*, 837−850.
(3) Hu, J.; Zhu, Y.; Huang, H.; Lu, J. *Prog. Polym. Sci.* **2012**, *37*, 1720−1763.
(4) Liu, C.; Qin, H.; Mather, P. T. *J. Mater. Chem.* **2007**, *17*, 1543−1558.
(5) Miaudet, P.; Derré, A.; Maugey, M.; Zakri, C.; Piccione, P. M.; Inoubli, R.; Poulin, P. *Science* **2007**, *318*, 1294−1296.
(6) Kratz, K.; Madbouly, S. A.; Wagermaier, W.; Lendlein, A. *Adv. Mater.* **2011**, *23*, 4058−4062.
(7) Viry, L.; Mercader, C.; Miaudet, P.; Zakri, C.; Derré, A.; Kuhn, A.; Maugey, M.; Poulin, P. *J. Mater. Chem.* **2010**, *20*, 3487−3495.
(8) Xie, T. *Nature* **2010**, *464*, 267−270.
(9) Li, J.; Xie, T. *Macromolecules* **2011**, *44*, 175−180.
(10) Luo, Y.; Guo, Y.; Gao, X.; Li, B.-G.; Xie, T. *Adv. Mater.* **2013**, *25*, 743−748.
(11) Leng, J.; Lan, X.; Liu, Y.; Du, S. *Prog. Mater. Sci.* **2011**, *56*, 1077−1135.
(12) Meng, Q.; Hu, J.; Zhu, Y. *J. Appl. Polym. Sci.* **2007**, *106*, 837−848.
(13) Meng, Q.; Hu, J. *Compos. Part Appl. Sci. Manuf.* **2009**, *40*, 1661−1672.
(14) Razzaq, M. Y.; Behl, M.; Lendlein, A. *Adv. Funct. Mater.* **2012**, *22*, 184−191.
(15) Gall, K.; Dunn, M. L.; Liu, Y.; Stefanic, G.; Balzar, D. *Appl. Phys. Lett.* **2004**, *85*, 290−292.
(16) Meng, H.; Li, G. *Polymer* **2013**, *54*, 2199−2221.
(17) Xie, T. *Polymer* **2011**, *52*, 4985−5000.
(18) Sun, L.; Huang, W. M. *Soft Matter* **2010**, *6*, 4403−4406.
(19) Zhao, Q.; Behl, M.; Lendlein, A. *Soft Matter* **2013**, *9*, 1744−1755.
(20) Kunzelman, J.; Chung, T.; Mather, P. T.; Weder, C. *J. Mater. Chem.* **2008**, *18*, 1082−1086.
(21) Luo, X.; Mather, P. T. *Soft Matter* **2010**, *6*, 2146−2149.
(22) Grillard, F.; Jaillet, C.; Zakri, C.; Miaudet, P.; Derré, A.; Korzhenko, A.; Gaillard, P.; Poulin, P. *Polymer* **2012**, *53*, 183−187.
(23) Onsager, L. *Ann. N.Y. Acad. Sci.* **1949**, *51*, 627−659.
(24) Balberg, I.; Anderson, C. H.; Alexander, S.; Wagner, N. *Phys. Rev. B* **1984**, *30*, 3933−3943.
(25) Sheng, P. *Phys. Rev. B* **1980**, *21*, 2180−2195.
(26) Sheng, P.; Sichel, E. K.; Gittleman, J. I. *Phys. Rev. Lett.* **1978**, *40*, 1197−1200.
(27) Li, C.; Thostenson, E. T.; Chou, T.-W. *Appl. Phys. Lett.* **2007**, *91*, 223114.
(28) Kyrylyuk, A. V.; Hermant, M. C.; Schilling, T.; Klumperman, B.; Koning, C. E.; van der Schoot, P. *Nat. Nanotechnol.* **2011**, *6*, 364−369.
(29) Dencheva, N.; Nunes, T. G.; Oliveira, M. J.; Denchev, Z. *J. Polym. Sci., Part B: Polym. Phys.* **2005**, *43*, 3720−3733.

(30) Inoue, K.; Hoshino, S. *J. Polym. Sci., Polym. Phys. Ed.* **1973**, *11*, 1077−1089.
(31) Miaudet, P.; Bartholome, C.; Derré, A.; Maugey, M.; Sigaud, G.; Zakri, C.; Poulin, P. *Polymer* **2007**, *48*, 4068−4074.
(32) Badaire, S.; Pichot, V.; Zakri, C.; Poulin, P.; Launois, P.; Vavro, J.; Guthy, C.; Chen, M.; Fischer, J. E. *J. Appl. Phys.* **2004**, *96*, 7509.
(33) Vigolo, B.; Poulin, P.; Lucas, M.; Launois, P.; Bernier, P. *Appl. Phys. Lett.* **2002**, *81*, 1210.
(34) Du, F.; Fischer, J. E.; Winey, K. I. *Phys. Rev. B* **2005**, *72*, 121404.
(35) Balberg, I.; Binenbaum, N.; Wagner, N. *Phys. Rev. Lett.* **1984**, *52*, 1465−1468.
(36) Perrot, C.; Piccione, P. M.; Zakri, C.; Gaillard, P.; Poulin, P. *J. Appl. Polym. Sci.* **2009**, *114*, 3515−3523.
(37) Miaudet, P.; Badaire, S.; Maugey, M.; Derré, A.; Pichot, V.; Launois, P.; Poulin, P.; Zakri, C. *Nano Lett.* **2005**, *5*, 2212−2215.